Article

Not peer-reviewed version

A Structural Colored Epoxy Resin Sensor for the Discrimination of Methanol and Ethanol

Yongxing Guo , Yingying Yi , Limin Wu , Wei Liu , Yi Li , Yonggang Yang *

Posted Date: 16 June 2025

doi: 10.20944/preprints202506.1272.v1

Keywords: epoxy resin; optical sensor; methanol detection; colorful pattern; cholesteric liquid crystal polymer network doi:10.20944/preprints202506.1272.v1

Article

A Structural Colored Epoxy Resin Sensor for the Discrimination of Methanol and Ethanol

Yongxing Guo [1], Yingying Yi [1], Limin Wu [2], Wei Liu [1], Yi Li [1] and Yonggang Yang [1,*]

[1] State and Local Joint Engineering Laboratory for Novel Functional Polymeric Materials, Department of Polymer Science and Engineering, College of Chemistry, Chemical Engineering and Materials Science, Soochow University, Suzhou 215123, China
[2] School of Environmental Science and Engineering, Yancheng Institute of Technology, Yancheng, Jiangsu Province, P. R. China
* Correspondence: ygyang@suda.edu.cn (Y. Y.).

Abstract: A thermochromic cholesteric liquid crystal (CLC) mixture was prepared using epoxies. The structural color of the CLCN film was tuned by changing the concentration of a chiral dopant and the polymerization temperature. It was found the yellow CLCN film can be used as a sensor for the discrimination of methanol and ethanol which was proposed to be driven by the difference between the solubility parameters. Moreover, a colorful pattern was prepared based on the thermochromic property of the CLC mixture, which could be applied for decoration and as a sensor for chloroform.

Keywords: epoxy resin; optical sensor; methanol detection; colorful pattern; cholesteric liquid crystal polymer network

1. Introduction

Sensor technology is a technology that can respond to external stimuli with high sensitivity using electrochemical, optical and mass analysis methods [1,2]. Optical sensors offer the advantages of high sensitivity, ease of fabrication and handling, simple quantification and visual recognition by the naked eye. For these reasons, the optical sensors have become an attractive class of sensors [3]. Optical sensors can be developed by mimicking the Bragg reflection properties of ordered periodic structures those can reflect visible light in nature [4–6]. Since the photonic crystals can reflect light with the specific wavelengths in the visible range, the optical sensors prepared using photonic crystals can detect analytes by color change without a power source [7–9].

Among the photonic crystals, the cholesteric liquid crystal (CLC) with a helical supramolecular structure attracts much attention [10–13]. Since the selective Bragg reflection band wavelength of CLC is sensitive to various external stimuli, the reflective wavelength can be adjusted [14–22]. The CLC polymer network (CLCN) sensor is displayed as a solid film, the simple structure and high thermostability have attracted the attention of many researchers [23–33]. Therefore, CLCN film is an excellent choice for the preparation of optical sensors. These sensors can be used to detect pH [23–25], humidity [26,27], metal ions [28–30] and gasses [31–33]. The chemicals penetrate into the CLCN framework, resulting in a change of the helical pitch [19].

Methanol can cause serious damage to the human body, and the high degree of similarity between methanol and ethanol makes the identification of them challenging [34]. Various methods to distinguish between methanol and ethanol have been reported, such as gas chromatography-mass spectrometry [35], Raman spectroscopy [36], optical fiber sensing [37–39], electrochemical methods [40] and multifunctional nanomaterials [41]. For the discrimination of methanol and ethanol, a hydrogen bridged CLCN film with porosity was prepared [15,17,34]. The sensing capability is enhanced by the porosity. Since the CLCN film should be treated with alkali to activate the hydrogen bonds, it is not suitable for large-area preparation. Most of the previously reported CLCN sensors were prepared based on polyacrylates. The free radical polymerization of acrylate monomers suffers from oxygen inhibition [42–44]. Therefore, the polyacrylate-based CLCN films are generally prepared in a nitrogen atmosphere [19,44]. However, the cationic polymerization of the epoxy monomers does not suffer from oxygen inhibition [45–47]. Therefore, epoxy resin-based CLCN films are attractive for potential applications. Herein, an epoxy resin-based CLCN film was prepared. The structural color of the CLCN film was tuned by changing the concentration of a chiral dopant and the polymerization temperature. The yellow CLCN film can act as a sensor for the discrimination of methanol and ethanol. Moreover, a colorful pattern was prepared based on the thermochromic property of the CLC mixture, which could be applied for decoration and as a sensor for chloroform.

2. Materials and Methods

2.1. Chemical Reagents and Instruments

E11M and CA-Epoxy were synthesized according to the literatures [47,48]. Tetrahydrofuran (THF) was obtained from Shanghai Lingfeng Chemical Reagent Co., Ltd. Photoinitiators 1176 and ITX, and Syna-Epoxy 06E were purchased from Shanghai Aladdin Biochemical Technology Co., Ltd. All other reagents were purchased from Sinopharm Group Chemical Reagent Co., Ltd. and used as received without further purification. The rubbing-oriented poly(ethylene terephthalate) (PET) film was given by Nanya plastics Co., Ltd. The photomasks for the patterns were obtained by printing the picture on the surface of a PET film using the printer HP LaserJet P1007.

The polarized optical microscopy (POM) image of the CLC mixture was taken using a CPV-900C polarization microscope fitted with a Linkam LTS420 hot stage (Linkam Scientific Instruments, UK). Differential scanning calorimetry (DSC) measurements were conducted on a TA-Q200 (TA Instruments, New Castle, DE, USA) under nitrogen at 10.0 °C min^{-1}. The field-emission scanning electron microscopy (FE-SEM) images were taken using a Hitachi Regulus-8230 (HITACHI, Tokyo, Japan) operating at 5.0 kV. The UV–Vis–NIR spectra were obtained with a UV–Vis spectrophotometer (UV1900i, SHIMADZU, Kyoto, Japan). The circular dichroism (CD) spectra were measured using a JASCO 815 spectrometer (JASCO, Tokyo, Japan). The UV LED series equipment (UVSF81T) was produced by FUTANSI Electronic Technology Co., Ltd (Shanghai, China). The UV LED parallel light source is equipped with double aspherical quartz lenses to produce parallel light with a parallel half angle of less than 2°. Thermogravimetric analysis (TGA) of an epoxy resin film was performed using TG/DTA 6300 (HITACHI, Tokyo, Japan) under nitrogen at 10.0 C min^{-1}. The A4UV printer was purchased from Shenzhen Songpu Industrial Group Co., Ltd (Shenzhen, China).

2.2. Preparation of the Structurally Colored CLCN Films

A typical preparation procedure is shown as follows. A mixture of E11M/CA-Epoxy/Syna-Epoxy 06E/ITX/1176 was prepared at the weight ratio of 80.4/4.6/10.0/2.0/3.0, which was dissolved in a cyclopentanone/cyclohexanone (v/v, 4:1) mixture at a solid content of 20 wt%. The solution was coated on the surface of a PET film using a 20-μm Mayer bar. After removing the solvents, the CLC mixture was photopolymerized at 90 °C under the irradiation of the 365-nm LED lamp (400 mW cm^{-2}) for 5.0 s and then held at 90 °C for 12 h, subsequently. Finally, a CLCN film was obtained. The other CLCN films were prepared by changing the weight ratios of CA-Epoxy and temperatures.

2.3. Preparation of the CLCN Patterns at Different Temperatures

A typical preparation procedure is shown as follows. A mixture of E11M/CA-Epoxy/Syna-Epoxy 06E/ITX/1176 was prepared at the weight ratio of 80.4/4.6/10.0/2.0/3.0. The CLC mixture was coated on the surface of a PET film as above. Then, photopolymerization was carried out at 95 °C under the irradiation of the 365-nm LED lamp (400 mW cm^{-2}) for 5.0 s through a photomask with an octopus or a beetle image. After removing the photomask, the film was cooled down to 60 °C. Finally, the colorful pattern was obtained under the irradiation of the 365-nm LED lamp (400 mW cm^{-2}) for 5.0 s and then held at 90 °C for 12 h. Another CLCN film with an octopus pattern was prepared at E11M/CA-Epoxy/Syna-Epoxy 06E/ITX/1176 weight ratio of 79.0/6.0/10.0/2.0/3.0.

2.4. Preparation of the Lizard Pattern Using the Inkjet Printer

Four color CLC inks were prepared at the E11M/CA-Epoxy/Syna-Epoxy 06E/ITX/1176 weight ratios of 81.2/3.8/10.0/2.0/3.0, 80.8/4.2/10.0/2.0/3.0, 80.4/4.6/10.0/2.0/3.0 and 79.6/5.4/10.0/2.0/3.0, respectively, which were dissolved in the cyclohexanone/*N*,*N*-dimethylacetamide (DMAC) (v/v, 4/6) mixture to form transparent solutions with a solid content of 20 wt%. After the lizard pattern was printed, the solvents were removed at 90 °C. Then, photopolymerization was carried out at 90 °C under the irradiation of the 365-nm LED lamp (400 mW cm^{-2}) for 5.0 s and then held at 90 °C for 12 h.

3. Results and Discussion

The molecular structures of E11M and CA-Epoxy are shown in (Figure 1). E11M shows an enantiotropic nematic phase with the phase transition sequence of Cr$_1$ 67.5 °C Cr$_2$ 75.3 °C N 147.9 °C I 146.0 °C N 49.2 °C Recr (Cr, crystal; N, nematic phase; I, isotropic phase; Recr, recrystal) [47]. CA-Epoxy is a chiral dopant, which has been applied for the preparation of CLC mixtures [48]. The melting point is 134.8 °C (Figure S1). 1176 acts as the cationic photoinitiator, and ITX acts as the co-photoinitiator. Radical initiators are generally used as the co-initiators to accelerate the polymerization rate of epoxyethane [49]. ITX molecules can be used to form radicals under UV irradiation, and then the radicals can be oxidized by 1176 to form carbon cations [47]. Then, the carbon cations trigger the polymerization of the epoxy group. The addition of Syna-Epoxy O6E can increase the rate of polymerization of epoxy resins without phase separation [50]. For the E11M/CA-Epoxy/Syna-Epoxy 06E/ITX/1176 mixture prepared at the weight ratio of 80.4/4.6/10.0/2.0/3.0, a Grandjean texture was identified in the POM image taken at 90 °C during the cooling process, indicating a cholesteric structure (Figure S2).

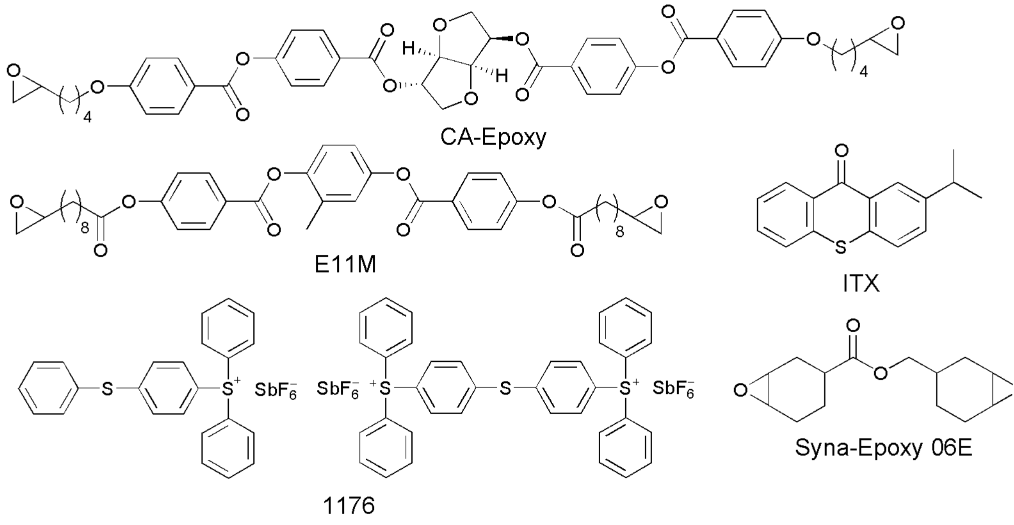

Figure 1. Molecular structures of the compounds.

Since the alignment of the LC molecules plays an important role in eliminating the defects of cholesteric phase, herein, the rubbing-oriented PET film was used as the substrate. Due to the chain transfer reaction between water and epoxy, the cross-linking density will be decreased with the existence of water. Herein, the cationic polymerization was carried out subsequently after removing the solvents at a hot temperature to avoid of absorbing of water from air [51,52]. Moreover, in order to ensure the thorough cross-linking of the framework, the thermo-treatment was carried out at 90 °C after photopolymerization. With the increase in the concentration of CA-Epoxy from 3.8 to 5.8 wt% (Table S1), the structural color of the CLCN film changed from red to purple (Figure 2a). The wavelength at the maximum of reflection band shifted from 645 to 425 nm (Figure 2b). Due to the specular reflection and light scattering, the baselines of the spectra were about 87 %. The optical activity of the CLCN films was characterized by taking CD spectra (Figure 2c). Since all of the CD signals were negative, the epoxy resin films should form a right-handed supramolecular helical structure. The microstructure of the CLCN films was studied using FE-SEM. The helical pitch of the CLCN films prepared at the CA-Epoxy concentration of 3.8 and 5.8 wt% were 392 and 265 nm, respectively (Figure S3). The TGA curve of the CLCN film prepared using 4.6 wt% of CA-Epoxy indicated that the starting decomposition temperature of an epoxy resin film was about 348 °C (Figure S4). Therefore, the CLCN film has a high thermo-stability.

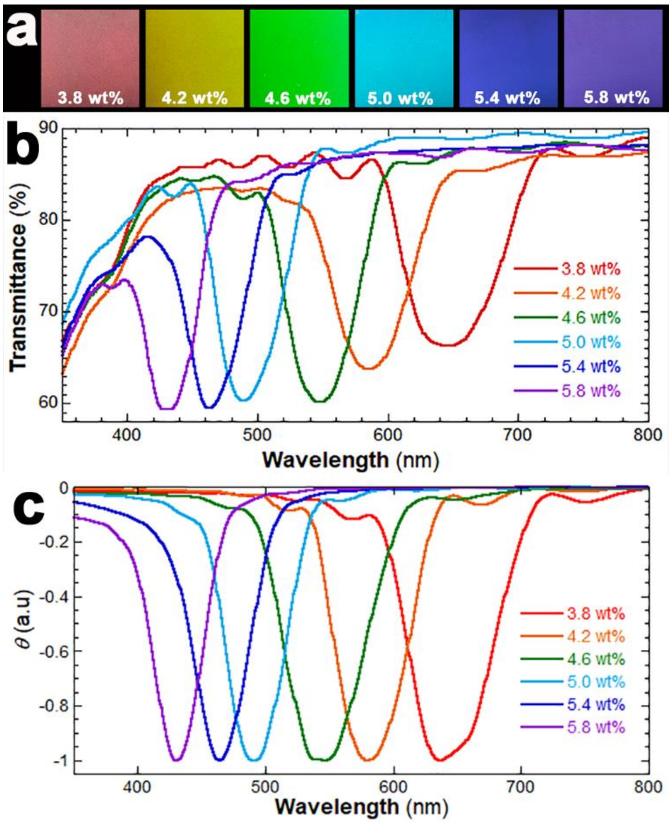

Figure 2. (a) Photographs, (b) UV–Vis spectra and (c) CD spectra of the CLCN films prepared at different CA-Epoxy concentrations.

The CLC mixture prepared at the CA-Epoxy concentration of 4.6 wt% showed a thermochromic property (Figure 3). With increasing the polymerization temperature from 50 to 95 °C, the color of the film changed from orange to green, and the wavelength at the maximum of reflection band shifted from 600 to 525 nm (Figure 3). Moreover, the intensity of the reflection band increased gradually. Therefore, it was possible to prepare colorful patterns based on this thermochromic property [47].

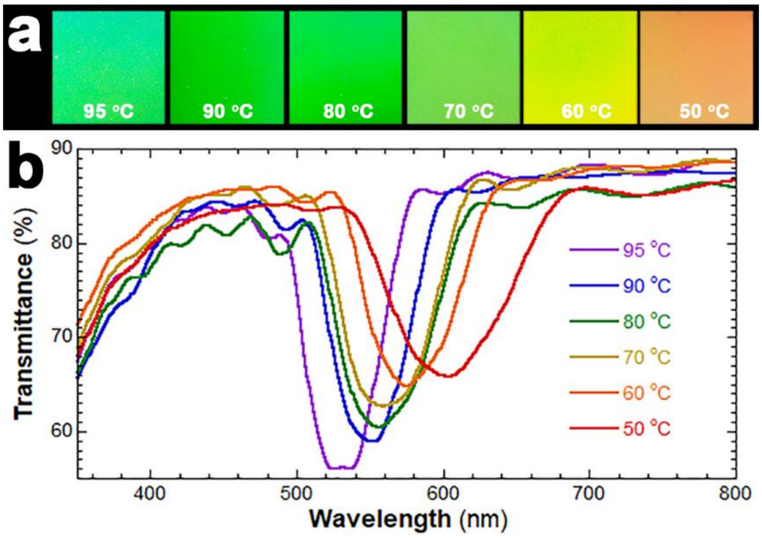

Figure 3. (a) Photographs and (b) UV–Vis spectra of the CLCN films prepared using a CLC mixture with 4.6 wt% of CA-Epoxy at different temperatures.

Based on the thermochromic property of the CLC mixture, both a beetle picture and an octopus one were prepared using different masks (Figure 4). The structural color was controlled by changing the polymerization temperature. The preparation process of a patterned film is illustrated in Scheme 1. Firstly, the CLC mixture is coated on the surface of a rubbing-oriented PET film. A CLC film with a green structural color is obtained at 95 °C. Then, photopolyermization is carried out under the irradiation of a 365-nm LED lamp (400 mW cm^{-2}) for 5.0 s through a photomask. After removing the photomask, the temperature of the film is cooled down to 60 °C. A colorful pattern is appeared. After photopolymerization, the patterned CLCN film is obtained.

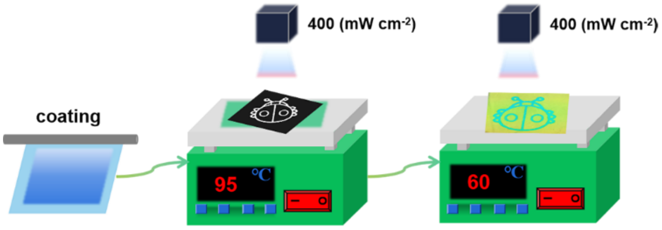

Scheme 1. Schematic representation of the preparation of patterned film.

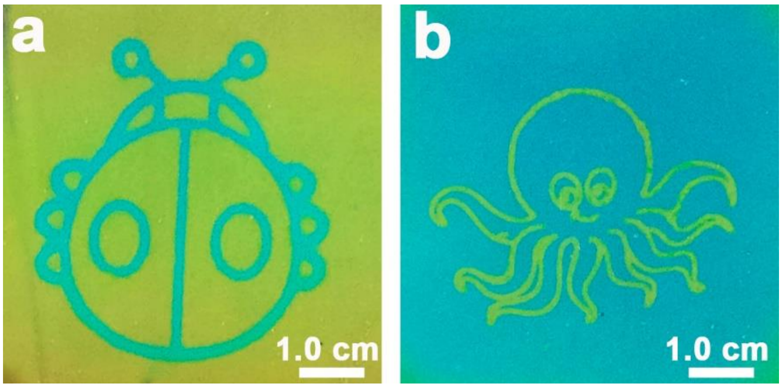

Figure 4. Photographs of the patterned CLCN films.

To study the solvatochromic property of the CLCN films, a yellow CLCN film was immersed in different solvents for 10 min to reach the adsorption-desorption equilibrium, which was prepared using 4.6 wt% of CA-Epoxy at 60 °C (Figure 5). The selective reflection band of the CLCN film shifted to the longer wavelength, due to the swelling of the film in the solvents. When the CLCN film was immersed in ethanol, although the selective reflection band shifted from 575 to 585 nm, the yellow color was kept. However, when the CLCN film was immersed in methanol, the elective reflection band shifted to 600 nm, and the color of the CLCN film changed to orange. This structural color change could be clearly identified by the naked eye. Due to the different swelling ability of ethanol and methanol, this CLCN film can be used as a sensor for the discrimination of them. It was reported that the thermal post-curing played an important role in increasing the cross-linking density of epoxy resins [53]. For the CLCN film prepared without thermal post-curing, the selective Bragg reflection band shifted from 570 to 610 nm, after it was immersed in methanol (Figure S5). Therefore, the cross-linking density played an important role in this swelling. The stability of the thermal post-curing CLCN film was studied by immersing it into methanol and then removing it for ten times (Figure S6). It was found that the wavelengths of the Bragg reflection band of the dried and swelled CLCN film were stable.

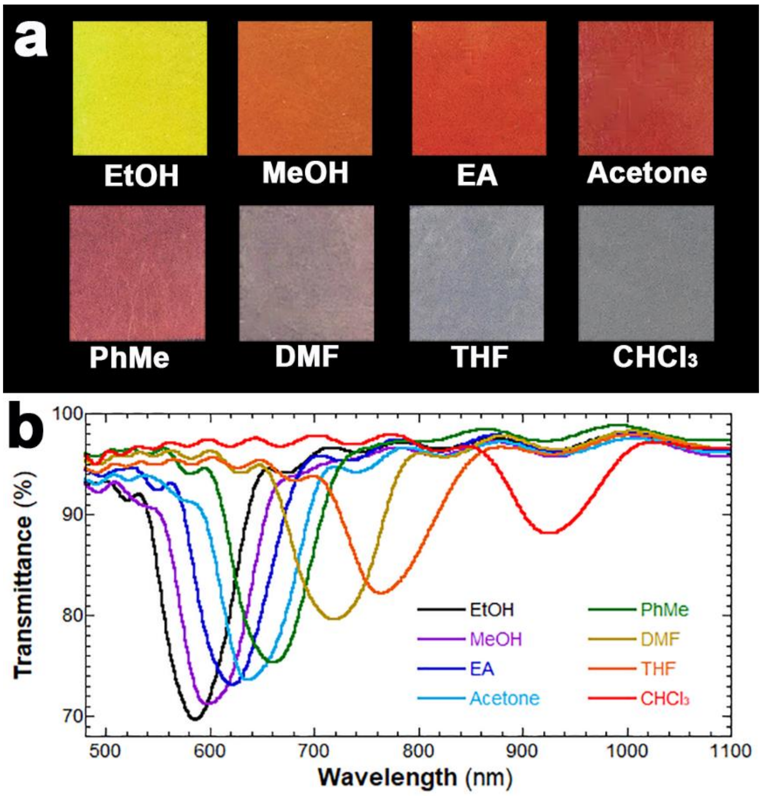

Figure 5. (a) Photographs and (b) UV UV–Vis–NIR spectra of the CLCN film in different solvents.

When the CLCN film was immersed in ethyl acetate (EA), acetone or toluene, the color changed to red. And when the CLCN film was immersed in *N*,*N*-dimethyl formamide (DMF), the color changed to pale red. And when the CLCN film was immersed in tetrahydrofuran (THF) or chloroform, the film became colorless. The solubility parameters of the solvents should play an important role in the swelling ability [54]. The Hansen solubility parameters of ethanol, methanol, EA, acetone, toluene, DMF, THF and chloroform are 26.5, 29.6, 18.1, 20.0, 18.2, 24.8, 19.4 and 19.0 $MPa^{0.5}$, respectively. The backbone and the terminal of the epoxy resin have an ether structure and a hydroxyl group, respectively. The Hansen solubility parameters of diethylene glycol monoethyl ether and diethylene glycol are 22.0 and 29.9 $MPa^{0.5}$, respectively. The swelling of the epoxy resin should be driven by the intermolecular hydrogen bonding and dipole-dipole forces [15].

To further reveal the discrimination of ethanol and methanol, the CLCN film was immersed in the ethanol/methanol mixtures with different methanol fractions for 10 min (Figure 6). When the CLCN film was immersed in the methanol/ethanol (v/v, 6/4) mixture, eight minutes was enough to reach the adsorption-desorption equilibrium (Figure S7). It should be noted here that 5.0 vol% of methanol was enough for recognization by the naked eyes. With increasing the volume ratio of methanol/ethanol, the reflection band of the film gradually red-shifted, and reached a stable state at 60 vol% of methanol. The intermolecular bonding force was proposed to drive this phenomenon. The solvatochromic property of the CLCN film was also studied in the water/ethanol and water/methanol mixtures (Figure S8 and S9). The Bragg reflection band shifted to longer wavelength with increasing the methanol or ethanol concentration, and reached the stable state at about 70 wt% of methanol or 80 wt% of ethanol. The structural color of the CLCN film changed to red, when the methanol concentration reached 40 wt% (Figure S8a). However, it did not change much with increasing the ethanol concentration (Figure S9a).

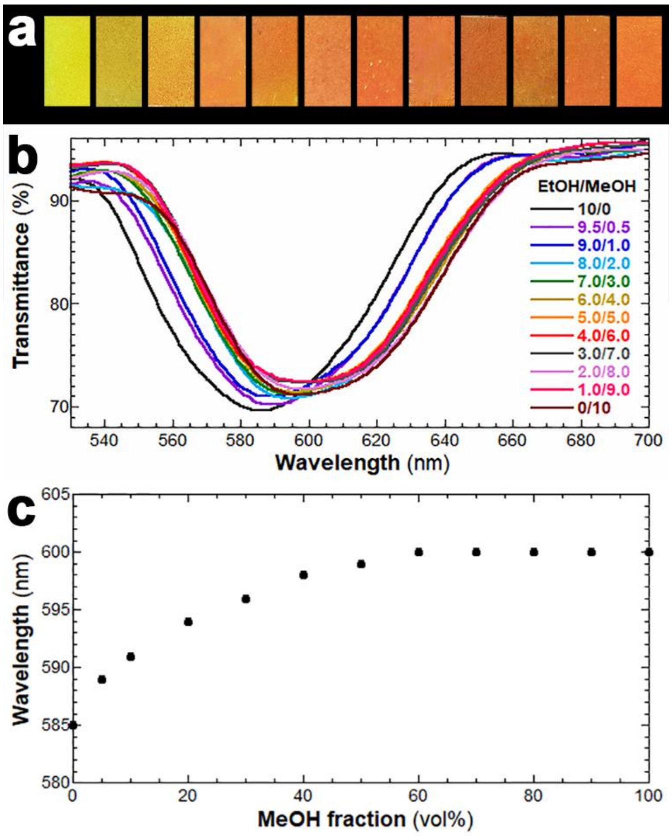

Figure 6. (a) Photographs, (b) UV–Vis spectra and (c) λ_{max} value of the UV–Vis absorption band of the CLCN film at different MeOH fractions.

Since chloroform is harmful to human body and the CLCN film shown here is sensitive to chloroform, a patterned sensor for chloroform was prepared using the E11M/CA-Epoxy/Syna-Epoxy 06E/ITX/1176 mixture prepared at the weight ratio of 79.0/6.0/10.0/2.0/3.0 and the polymerization temperatures of 60 and 90 °C (Figure 7a). The wavelengths of the reflection bands of the pattern and background areas were identified at 392 and 461 nm, respectively (Figure S10). After the CLCN was fumigated using chloroform, the background and the pattern turned to red and green, respectively (Figure 7b). Since the volatilization rate of chloroform is high at room temperature, the structural colors recovered within few seconds. Moreover, a lizard pattern was prepared using four CLC inks on the surface of a PET film through inkjet printing (Figure S11). The structural colors of the pattern were controlled by changing the chiral dopant concentration. Since the viscosities of the CLC mixtures were too high to be printed, a cyclohexanone/DMAC (v/v, 4/6) mixture was added into the CLC mixtures. Therefore, the epoxy resin-based CLCN films with the solvatochromic property can be applied not only as sensors for chemicals, but also for decorations.

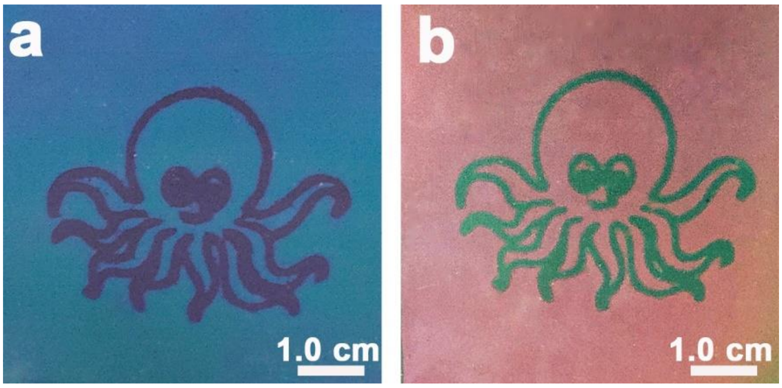

Figure 7. Photographs of the patterned CLCN film exposed to (a) air and (b) chloroform vapor, respectively.

4. Conclusions

CLCN films with a structural color were prepared using an epoxy liquid crystal and a chiral additive through photopolymerization. The structural color was controlled by changing the concentration of the chiral additive and the polymerization temperature. The solvatochromic property of the CLCN film with a yellow structural color was studied. It was found that this film can discriminate methanol and ethanol. This phenomenon was proposed to be caused by the difference between the solubility parameters of methanol and ethanol. Based on the thermochromic property of the CLC mixture, colorful patterns were prepared, which could be applied for decoration and as sensors for chemicals.

Supplementary Materials: The following supporting information can be downloaded at the website of this paper posted on Preprints.org, Table S1 Weight ratios of the compounds in the CLC mixtures; Figure S1: DSC curves of CA-Epoxy; Figure S2: POM image of the E11M/CA-Epoxy/Syna-Epoxy 06E/ITX/1176 (w/w/w/w/w, 80.4/4.6/10.0/2.0/3.0) mixture taken at 90.0 °C during the cooling process; Figure S3: FE-SEM images of the cross-sections of the CLCN films prepared with (a) 3.8 wt% and (b) 5.8 wt% of CA-Epoxy; Figure S4: TGA curve of the epoxy resin prepared at the E11M/CA-Epoxy/Syna-Epoxy 06E/ITX/1176 weight ratio of 80.4/4.6/10.0/2.0/3.0; Figure S5: UV–Vis spectra of the CLCN film prepared at the E11M/CA-Epoxy/Syna-Epoxy 06E/ITX/1176 weight ratio of 80.4/4.6/10.0/2.0/3.0 and without thermal post-curing; Figure S6: λ_{max} values of the CLCN film after being immersed in methanol and dried for ten times; Figure S7: Time-dependent (a) photographs, (b) UV–Vis spectra and (c) λ_{max} values of the CLCN film immersed in the methanol/ethanol (v/v, 6/4) mixture; Figure S8: (a) Photographs, (b) UV–Vis spectra and (c) λ_{max} value of the UV–Vis absorption band of the CLCN film at different MeOH fractions; Figure S9: (a) Photographs, (b) UV–Vis spectra and (c) λ_{max} value of the UV–Vis absorption band of the CLCN film at different EtOH fractions; Figure S10: UV–Vis spectra of the colorful pattern; Figure S11: Lizard pattern prepared through inkjet printing.

Author Contributions: Conceptualization, Y.Y.; investigation, Y.G. and Y.Y.; writing–original draft preparation, Y.G., Y.L. and W.L.; writing–review and editing, W.L. and Y.Y.; supervision, Y.Y.; project administration, Y.L. and Y.Y.; funding acquisition, Y.Y. All authors have read and agreed to the published version of the manuscript.

Author Contributions: This work was supported by the National Natural Science Foundation of China (No. 52273212), Jiangsu Engineering Laboratory of Novel Functional Polymeric Materials, Jiangsu Key Laboratory of Advanced Functional Polymer Materials, Key Laboratory of Polymeric Materials Design and Synthesis for Biomedical Function.

Data Availability Statement: The original contributions presented in the study are included in the article/Supplementary Materials, and further inquiries can be directed to the corresponding author.

Conflicts of Interest: The authors declare no conflicts of interest.

References

1. Holtz, J. H.; Asher, S. A. Polymerized Colloidal Crystal Hydrogel Films as Intelligent Chemical Sensing Materials. *Nature* **1997**, *389*, 829–832.
2. Noh, K.-G.; Park, S.-Y. Biosensor Array of Interpenetrating Polymer Network with Photonic Film Templated from Reactive Cholesteric Liquid Crystal and Enzyme-Immobilized Hydrogel Polymer. *Adv. Funct. Mater.* **2018**, *28*, 1707562.
3. 3.Fujii, Y.; Honma, S.; Morisawa, M.; Muto, S. Development of New Optical Fiber Toluene Sensor. *Adv. Mater. Devices Sens. Imaging III* **2007**, *6829*, 68291Z.
4. Bikbaev, R. G.; Timofeev, I. V.; Shabanov, V. F. Strain Sensor via Wood Anomalies in 2D Dielectric Array. *Nanomaterials* **2021**, *11*, 1022.
5. Batir, O.; Bat, E.; Bukusoglu, E. Strain-Enhanced Sensitivity of Polymeric Sensors Templated from Cholesteric Liquid Crystals. *Soft Matter* **2020**, *16*, 6794–6802.
6. Boyon, C.; Soldan, V.; Mitov, M. Bioinspired, Cholesteric Liquid-Crystal Reflectors with Time-Controlled Coexisting Chiral and Achiral Structures. *ACS Appl. Mater. Interfaces* **2021**, *13*, 30118–30126.
7. Wang, H.; Zhang, K.-Q. Photonic Crystal Structures with Tunable Structure Color as Colorimetric Sensors. *Sensors* **2013**, *13*, 4192–4213.
8. Fenzl, C.; Hirsch, T.; Wolfbeis, O. S. Photonic Crystals for Chemical Sensing and Biosensing. *Angew. Chem., Int. Ed.* **2014**, *53*, 3318–3335.
9. Ge, J.; Yin, Y. Responsive Photonic Crystals. *Angew. Chem., Int. Ed.* **2011**, *50*, 1492–1522.
10. Zhang, D.; Cao, H.; Duan, M.; Wang, H.; Chen, Y.; Zong, C.; Gan, P.; Zhao, L.; Yang, Z.; Wang, D.; He, W. Effect of Monomer Composition on the Performance of Polymer-Stabilized Liquid Crystals with Two-Step Photopolymerization. *J. Polym. Sci. Pol. Phys.* **2019**, *57*, 1126–1132.
11. Mitov, M. Cholesteric Liquid Crystals with a Broad Light Reflection Band. *Adv. Mater.* **2012**, *24*, 6260–6276.
12. Dierking, I. Recent Developments in Polymer Stabilised Liquid Crystals. *Polym. Chem.* **2010**, *1*, 1153–1159.
13. Ye, Y.; Guo, L.; Zhong, T. A Review of Developments in Polymer Stabilized Liquid Crystals. *Polymers* **2023**, *15*, 2962.
14. Tang, J.; Fang, J.; Liang, Y.; Zhang, B.; Chen, Z.; Liu, X.; Li, Z.; Cai, X.; Xian, J.; Lin, H.; Zhu, W.; Guan, H.; Lu, H.; Zhang, J.; Yu, J. All-Fiber-Optic Voc Gas Sensor Based on Side-Polished Fiber Wavelength Selectively Coupled with Cholesteric Liquid Crystal Film. *Sensor. Actuat. B-Chem.* **2018**, *273*, 1816–1826.
15. Chang, C.-K.; Bastiaansen, C. W. M.; Broer, D. J.; Kuo, H.-L. Discrimination of Alcohol Molecules Using Hydrogen-Bridged Cholesteric Polymer Networks. *Macromolecules* **2012**, *45*, 4550–4555.
16. Zhang, P.; Kragt, A. J. J.; Schenning, A. P. H. J.; de Haan, L. T.; Zhou, G. An Easily Coatable Temperature Responsive Cholesteric Liquid Crystal Oligomer for Making Structural Colour Patterns. *J. Mater. Chem. C* **2018**, *6*, 7184–7187.
17. Chang, C.-K.; Bastiaansen, C. M. W.; Broer, D. J.; Kuo, H.-L. Alcohol-Responsive, Hydrogen-Bonded, Cholesteric Liquid-Crystal Networks. *Adv. Funct. Mater.* **2012**, *22*, 2855–2859.
18. Lugger, S. J. D.; Houben, S. J. A.; Foelen, Y.; Debije, M. G.; Schenning, A. P. H. J.; Mulder, D. J. Hydrogen-Bonded Supramolecular Liquid Crystal Polymers: Smart Materials with Stimuli-Responsive, Self-Healing, and Recyclable Properties. *Chem. Rev.* **2022**, *122*, 4946–4975.
19. Herzer, N.; Guneysu, H.; Davies, D. J. D.; Yildirim, D.; Vaccaro, A. R.; Broer, D. J.; Bastiaansen, C. W. M.; Schenning, A. P. H. J. Printable Optical Sensors Based on H-Bonded Supramolecular Cholesteric Liquid Crystal Networks. *J. Am. Chem. Soc.* **2012**, *134*, 7608–7611.
20. Liu, B.; Yang, T.; Mu, X.; Mai, Z.; Li, H.; Wang, Y.; Zhou, G. Smart Supramolecular Self-Assembled Nanosystem: Stimulus-Responsive Hydrogen-Bonded Liquid Crystals. *Nanomaterials* **2021**, *11*, 448.
21. Raynes, E. P.; Jia, X. The Measurement of Weak Chirality Using Nematic Liquid Crystals. *Liq. Cryst.* **2017**, *44*, 1960–1967.
22. Popov, P.; Honaker, L. W.; Mirheydari, M.; Mann, E. K.; Jákli, A. Chiral Nematic Liquid Crystal Microlenses. *Sci. Rep.* **2017**, *7*, 1603.
23. Shibaev, P. V.; Schaumburg, K.; Plaksin, V. Responsive Chiral Hydrogen-Bonded Polymer Composites. *Chem. Mater.* **2002**, *14*, 959–961.

24. Shen, C.; Wang, Z.; Huang, R.; Bao, J.; Li, Z.; Zhang, L.; Lan, R.; Yang, H. Humidity-Responsive Photonic Crystals with pH and SO2 Gas Detection Ability Based on Cholesteric Liquid Crystalline Networks. *ACS Appl. Mater. Interfaces* **2022**, *14*, 16764–16771.
25. Chen, F.; Guo, J.; Jin, O.; Wei, J. A Temperature and pH Double Sensitive Cholesteric Polymer Film from a Photopolymerizable Chiral Hydrogen-Bonded Assembly. *Chin. J. Polym. Sci.* **2013**, *31*, 630–640.
26. Stumpel, J. E.; Broer, D. J.; Schenning, A. P. H. J. Water-Responsive Dual-Coloured Photonic Polymer Coatings Based on Cholesteric Liquid Crystals. *RSC Adv.* **2015**, *5*, 94650–94653.
27. Chen, F.; Guo, J.; Qu, Z.; Wei, J. Novel Photo-Polymerizable Chiral Hydrogen-Bonded Self-Assembled Complexes: Preparation, Characterization and the Utilization as a Thermal Switching Reflective Color Film. *J. Mater. Chem.* **2011**, *21*, 8574–8582.
28. Myung, D.-B.; Hussain, S.; Park, S.-Y. Photonic Calcium and Humidity Array Sensor Prepared with Reactive Cholesteric Liquid Crystal Mesogens. *Sensor. Actuat. B-Chem.* **2019**, *298*, 126894.
29. Moirangthem, M.; Arts, R.; Merkx, M.; Schenning, A. P. H. J. An Optical Sensor Based on a Photonic Polymer Film to Detect Calcium in Serum. *Adv. Funct. Mater.* **2016**, *26*, 1154–1160.
30. Stroganov, V.; Ryabchun, A.; Bobrovsky, A.; Shibaev, V. A Novel Type of Crown Ether-Containing Metal Ions Optical Sensors Based on Polymer-Stabilized Cholesteric Liquid Crystalline Films. *Macromol. Rapid Commun.* **2012**, *33*, 1875–1881.
31. Han, Y.; Pacheco, K.; Bastiaansen, C. W. M.; Broer, D. J.; Sijbesma, R. P. Optical Monitoring of Gases with Cholesteric Liquid Crystals. *J. Am. Chem. Soc.* **2010**, *132*, 2961–2967.
32. Niu, X.; Zhong, Y.; Chen, R.; Wang, F.; Luo, D. Highly Sensitive and Selective Liquid Crystal Optical Sensor for Detection of Ammonia. *Opt. Express* **2017**, *25*, 13549–13556.
33. Mujahid, A.; Stathopulos, H.; Lieberzeit, P. A.; Dickert, F. L. Solvent Vapour Detection with Cholesteric Liquid Crystals-Optical and Mass-Sensitive Evaluation of the Sensor Mechanism. *Sensors* **2010**, *10*, 4887–4897.
34. Yeh, T.-Y.; Liu, M.-F.; Lin, R.-D.; Hwang, S.-J. Alcohol Selective Optical Sensor Based on Porous Cholesteric Liquid Crystal Polymer Networks. *Molecules* **2022**, *27*, 773.
35. Tiscione, N. B.; Alford, I.; Yeatman, D. T.; Shan, X. Ethanol Analysis by Headspace Gas Chromatography with Simultaneous Flame-Ionization and Mass Spectrometry Detection. *J. Anal. Toxicol.* **2011**, *35*, 501–511.
36. Xu, Q.; Ye, Q.; Cai, H.; Qu, R. Determination of Methanol Ratio in Methanol-Doped Biogasoline by a Fiber Raman Sensing System. *Sensor. Actuat. B-Chem.* **2010**, *146*, 75–78.
37. Su, Y.; Lan, Z.; Wang, J.; Zeng, L.; Zhou, D.; Peng, Z.; Sun, W.; Liu, Y. Optical Fiber Sensor for Determination of Methanol Ratio in Methanol-Doped Ethanol Based on Two Cholesteric Liquid Crystal Droplets Embedded in Chitosan. *J. Lightwave Technol.* **2021**, *39*, 5170–5176.
38. Iqbal, F.; Biswas, S.; Bulbul, A. A.-M.; Rahaman, H.; Hossain, M. B.; Rahaman, M. E.; Awal, M. A. Alcohol Sensing and Classification Using PCF-based Sensor. *Sens. Bio-Sens. Res.* **2020**, *30*, 100384.
39. Liu, D.; Kumar, R.; Wei, F.; Han, W.; Mallik, A. K.; Yuan, J.; Wan, S.; He, X.; Kang, Z.; Li, F.; Yu, C.; Farrell, G.; Semenova, Y.; Wu, Q. High Sensitivity Optical Fiber Sensors for Simultaneous Measurement of Methanol and Ethanol. *Sensor. Actuat. B-Chem.* **2018**, *271*, 1–8.
40. Ishihara, S.; Iyi, N.; Labuta, J.; Deguchi, K.; Ohki, S.; Tansho, M.; Shimizu, T.; Yamauchi, Y.; Sahoo, P.; Naito, M.; Abe, H.; Hill, J. P.; Ariga, K. Naked-Eye Discrimination of Methanol from Ethanol Using Composite Film of Oxoporphyrinogen and Layered Double Hydroxide. *ACS Appl. Mater. Interfaces* **2013**, *5*, 5927–5930.
41. Yan, W.; Chen, Y.; Zeng, X.; Wu, G.; Jiang, W.; Wei, D.; Ling, M.; Ng, K. W.; Qin, Y. Ultrasensitive Ethanol Sensor Based on Segregated ZnO-In_2O_3 Porous Nanosheets. *Appl. Surf. Sci.* **2021**, *535*, 147697.
42. Lub, J.; Nijssen, W. P. M.; Wegh, R. T.; De Francisco, I.; Ezquerro, M. P.; Malo, B. Photoisomerizable Chiral Compounds Derived from Isosorbide and Cinnamic Acid. *Liq. Cryst.* **2005**, *32*, 1031–1044.
43. O'Brien, A. K.; Cramer, N. B.; Bowman, C. N. Oxygen Inhibition in Thiol-Acrylate Photopolymerizations. *J. Polym. Sci., Part A: Polym. Chem.* **2006**, *44*, 2007–2014.
44. Lub, J.; Nijssen, W. P. M.; Wegh, R. T.; Vogels, J. P. A.; Ferrer, A. Synthesis and Properties of Photoisomerizable Derivatives of Isosorbide and Their Use in Cholesteric Filters. *Adv. Funct. Mater.* **2005**, *15*, 1961–1972.

45. Hoekstra, D. C.; van der Lubbe, B. P. A. C.; Bus, T.; Yang, L.; Grossiord, N.; Debije, M. G.; Schenning, A. P. H. J. Wavelength-Selective Photopolymerization of Hybrid Acrylate-Oxetane Liquid Crystals. *Angew. Chem. Int. Ed.* **2021**, *60*, 10935–10941.
46. Shen, W.; Wang, L.; Cao, Y.; Zhang, L.; Yang, Z.; Yuan, X.; Yang, H.; Jiang, T.; Chen, H. Cationic Photopolymerization of Liquid Crystalline Epoxide in Mesogenic Solvents and Its Application in Polymer-Stabilized Liquid Crystals. *Polymer* **2019**, *172*, 231–238.
47. Zhang, X.; Guo, Y.; Li, Y.; Liu, W.; Li, H.; Yang, Y. Colorfully Patterned Epoxy Resin Films with a Cholesteric Structure Prepared through a Photopolymerization Approach. *ACS Appl. Polym. Mater.* **2023**, *5*, 193–200.
48. Guo, Y.; Zhao, J.; Li, Y.; Liu, W.; Yang, Y. Preparation and Applications of the Epoxy Resin-Based Polymer-Stabilised Cholesteric Liquid Crystal Films with Microcracks at the Surface. *Liq. Cryst.* **2023**, *50*, 2047–2058.
49. Hua, Y.; Crivello, J. V. Synergistic Interaction of Epoxides and *N*-Vinylcarbazole During Photoinitiated Cationic Polymerization. *J. Polym. Sci., Part A: Polym. Chem.* **2000**, *38*, 3697–3709.
50. Morita, Y. Cationic Polymerization of Hydrogenated Bisphenol-a Glycidyl Ether with Cycloaliphatic Epoxy Resin and Its Thermal Discoloration. *J. Appl. Polym. Sci.* **2005**, *97*, 1395–1400.
51. Walker, F. H.; Dickenson, J. B.; Hegedus, C. R.; Pepe, F. R.; Keller, R. New Polymeric Polyol for Thermoset Coatings: Superacid-Catalyzed Copolymerization of Water and Epoxy Resins. *J. Coat. Technol.* **2002**, *74*, 33–47.
52. Ge, X.; Ye, Q.; Song, L.; Misra, A.; Spencer, P. The Influence of Water on Visible-Light Initiated Free-Radical/Cationic Ring-Opening Hybrid Polymerization of Methacrylate/Epoxy: Polymerization Kinetics, Crosslinking Structure and Dynamic Mechanical Properties. *RSC Adv.* **2015**, *5*, 77791–77802.
53. Golaz, B.; Michaud, V.; Leterrier, Y.; Månson, J.-A.E. UV Intensity, Temperature and Dark-Curing Effects in Cationic Photo-Polymerization of a Cycloaliphatic Epoxy Resin. *Polymer* **2012**, *53*, 2038–2048.
54. Burke, J. Solubility Parameters: Theory and Application. **1984**.